Modeling the impact of heterogeneous reactions of chlorine on summertime nitrate formation in Beijing, China

Xionghui Qiu[1,2], Qi Ying[3*], Shuxiao Wang [1,2*], Lei Duan[1,2], Jian Zhao[4], Jia Xing[1,2], Dian Ding[1,2], Yele Sun[4], Baoxian Liu[5], Aijun Shi[6], Xiao Yan[6], Qingcheng Xu[1,2], Jiming Hao[1,2]

[1] State Key Joint Laboratory of Environmental Simulation and Pollution Control, School of Environment, Tsinghua University. Beijing 100084, China.

[2] State Environmental Protection Key Laboratory of Sources and Control of Air Pollution Complex, Beijing 100084, China

[3] Zachry Department of Civil Engineering, Texas A&M University, College Station, Texas 77843-3138, United States

[4] State Key Laboratory of Atmospheric Boundary Layer Physics and Atmospheric Chemistry, Institute of Atmospheric Physics, Chinese Academy of Sciences, Beijing 100029, China

[5] Beijing Environmental Monitoring Center, Beijing 100048, China

[6] Beijing Municipal Research Institute of Environmental Protection, Beijing 100037, China

*Corresponding author: shxwang@tsinghua.edu.cn & qying@civil.tamu.edu

Abstract:

A comprehensive chlorine heterogeneous chemistry is incorporated into the Community Multiscale Air Quality (CMAQ) model to evaluate the impact of chlorine-related heterogeneous reaction on diurnal and nocturnal nitrate formation and quantify the nitrate formation from gas-to-particle partitioning of HNO_3 and from different heterogeneous pathways. The results show that these heterogeneous reactions increase the atmospheric Cl_2 and $ClNO_2$ level (~100%), which further affect the nitrate formation. Sensitivity analyses of uptake coefficients show that the empirical uptake coefficient for the O_3 heterogeneous reaction with chlorinated particles may lead to the large uncertainties in the predicted Cl_2 and nitrate concentrations. The N_2O_5 uptake

coefficient with particulate Cl^- concentration dependence performs better to capture the concentration of $ClNO_2$ and nocturnal nitrate concentration. The reaction of OH and NO_2 in daytime increases the nitrate by ~15% when the heterogeneous chlorine chemistry is incorporated, resulting in more nitrate formation from HNO_3 gas-to-particle partitioning. By contrast, the contribution of the heterogeneous reaction of N_2O_5 to nitrate concentrations decreases by about 27% in the nighttime when its reactions with chlorinated particles are considered. However, the generated gas-phase $ClNO_2$ from the heterogeneous reaction of N_2O_5 and chlorine-containing particles further reacts with the particle surface to increase the nitrate by 6%. In general, this study highlights the potential of significant underestimation of daytime and overestimation of nighttime nitrate concentrations for chemical transport models without proper chlorine chemistry in the gas and particle phases.

1. Introduction

In recent years, nitrate has become the primary component of $PM_{2.5}$ (particulate matter with aerodynamic diameter less than 2.5μm) in Beijing with sustained and rapid reduction of SO_2 and primary particulate matter emissions (Ma et al., 2018; Li et al., 2018; Wen et al., 2018). Observations showed that the relative contributions of secondary nitrate in $PM_{2.5}$ could reach up to approximately 50% during some severe haze pollution days (Li et al., 2018). The mechanism of secondary nitrate formation can be summarized as two major pathways: (1) Gas-to-particle partitioning of HNO_3, which happens mostly in the daytime. The reaction of OH with NO_2 produces gaseous HNO_3, which subsequently partition into the particle phase. The existence of NH_3 or basic particles enhances this process by NH_3–NH_4^+ gas-particle equilibrium (Kleeman et al., 2005; Seinfeld and Pandis, 2006); (2) Hydrolysis of N_2O_5, which is more important at nighttime. N_2O_5 forms from the reactions of NO_2, O_3 and NO_3 and hydrolyzes to produce particulate nitrate. They can be summarized as reactions R1-R5 (Brown and Stutz 2012):

$$OH + NO_2 \rightarrow HNO_3 \qquad (R1)$$

$$HNO_3 + NH_3 \rightarrow NH_4^+ + NO_3^- \quad (R2)$$

$$NO_2 + O_3 \rightarrow NO_3 + O_2 \quad (R3)$$

$$NO_3 + NO_2 \leftrightarrow N_2O_5 \quad (R4)$$

$$N_2O_5 + H_2O(aq) \rightarrow 2H^+ + 2NO_3^- \quad (R5)$$

In addition to reactions R1 and R5, gas phase reactions of NO_3 with HO_2 and VOCs, N_2O_5 with water vapor (Tuazon et al., 1983) and the heterogeneous reaction of NO_2 with water-containing particle (Goodman et al., 1999) produce HNO_3 or nitrate as well. Theses reactions are listed in Table 2 as reactions R8, R9 and R10.

However, chemistry transport models (CTMs) incorporated with these mechanisms still can't accurately capture the spatiotemporal distributions of nitrate in some studies in polluted northern China. For example, Chang et al. (2018) showed that the simulated nitrate concentrations derived from the default CMAQ (version 5.0.2) were significantly higher than the observations in summer at two sites adjacent to Beijing. Fu et al. (2016) also found that default CMAQ (version 5.0.1) overestimated the simulated nitrate concentrations in the Beijing-Tianjin-Hebei region.

In recent fields studies, it was found that high particulate chlorine emissions might have a significant impact on the oxidation capacity of the urban atmosphere and thus could affect nitrate concentrations. According to the field measurements in June 2017 in Beijing (Zhou et al., 2018), the 2-min averaged concentrations of reactive molecular chlorine (Cl_2) and nitryl chloride ($ClNO_2$) reached up to 1000 pptv and 1200 pptv, respectively, during some severe air pollution periods in summer. The Cl_2 concentrations were significantly higher than those observed in North American coastal cities affected by onshore flow and the lower atmosphere in the remote Arctic region (Spicer et al., 1998; Glasow et al., 2010; Liu et al., 2017). During these pollution events, the corresponding concentrations of N_2O_5 (2-min average) and nitrate (5-min average) rose from 40 pptv and 1 μg m^{-3} to 700 pptv and 5 μg m^{-3}. To explain the high levels of $ClNO_2$, some studies suggested that reaction R5 should be revised to account for $ClNO_2$ production from the heterogeneous reaction of N_2O_5 on chloride-containing particles (CPS) (Osthoff et al., 2008; Thornton et al., 2010), as shown in reaction R6:

$$N_2O_5 + (1-\phi)\, H_2O + \phi\, Cl^- \rightarrow \phi\, ClNO_2 + (2-\phi)\, NO_3^- \quad (R6)$$

where ϕ represents the molar yield of $ClNO_2$. When Cl^- is enough, this reaction leads to lower nitrate concentrations than reaction R5. By incorporating this reaction into WRF-Chem, Li et al. (2016) found that the improved model performed better to match the observed nitrate concentrations in Hongkong during 15 November and 5 December 2013. However, $ClNO_2$ could affect the formation of nitrate indirectly by increasing the atmospheric OH after a series of chemical reactions, which are briefly summarized into three steps: (1) the photolysis of $ClNO_2$ produces chlorine radicals ($Cl^\bullet$); (2) the reaction of $Cl^\bullet$ with VOCs produces peroxy radical (HO_2 and RO_2); and (3) the increased HO_2 and RO_2 prompt the formation of OH through HOx cycle and lead to increased HNO_3 production (Young et al., 2014; Jobson et al., 1994). The overall impact of R6 on nitrate remains to be investigated.

Another related but unresolved issue is the sources of the high concentrations Cl_2, which could not be explained by the N_2O_5 heterogeneous reaction with Cl^- and the subsequent reactions of $ClNO_2$ in the gas phase. It has been reported that the reactions of gaseous O_3, OH, HO_2, $ClNO_2$, hypochlorous acid (HOCl), chlorine nitrate ($ClONO_2$) with CPS can produce Cl_2, which can subsequently photolyze to produce $Cl^\bullet$ (Knipping et al., 2000; George et al., 2010; Pratte et al., 2006; Deiber et al., 2004; Faxon et al., 2015). However, these heterogeneous reactions on CPS are generally missing in most of the current CTMs and it is unclear whether these reactions will be able to explain the observed Cl_2 concentrations and the overall impact of these reactions on nitrate.

Previously, biomass burning, coal combustion, and waste incineration were identified as the main sources of gaseous and particulate chlorine compounds in China from International Global Atmospheric Chemistry Program's Global Emissions Inventory Activity (GEIA) based on the year 1990 and a localized study by Fu et al. based on the year 2014 (Keene et al., 1999; Fu et al., 2018). However, recent source apportionment results of $PM_{2.5}$ in Beijing showed that the contribution of coal combustion had extremely decreased from 22.4% in 2014 to 3% in 2017 with the replacement of natural gas (obtained from official website of Beijing Municipal Bureau

of Statistics, available at http://edu.bjstats.gov.cn/). Another important source—cooking has received attention as its increasing contribution to $PM_{2.5}$ (accounting for 33% of the residential sector; obtained from the official source apportionment analysis of $PM_{2.5}$ in Beijing in 2017; see http://www.bjepb.gov.cn/bjhr-b/index/index.html). Moreover, the high content of particulate sodium chloride was measured from the source characterization studies of $PM_{2.5}$ released from the cooking activities (Zhang et al., 2016). Thus, it is necessary to compile an updated emission inventory for Beijing to include the emissions from cooking and other sources (coal burning, solid waste incineration, biomass burning, etc.) in order to explore the emissions of the chlorine species on atmospheric nitrate formation.

In this study, a CMAQ model with an improved chlorine heterogeneous chemistry is applied to simulate summer nitrate concentration in Beijing. Sensitivity simulations are conducted to evaluate the contributions of HNO_3 gas-to-particle partitioning and heterogonous production to aerosol nitrate. The results of this work can improve our understandings on nitrate formation and provide useful information on nitrate pollution control strategies in Beijing.

2. Emissions, chemical reactions and model description

2.1 Emissions

Generally, the conventional emission inventories of air pollutants in China only include the common chemical species, such as SO_2, NO_X, VOCs, $PM_{2.5}$, PM_{10}, NH_3, BC, and OC (Wang et al., 2014). Chloride compound emissions were not included. However, the emissions of chlorine species are vital for studying the chlorine chemical mechanism. Recently, the inorganic hydrogen chloride (HCl) and fine particulate chloride (PCl) emission inventories for the sectors of coal combustion, biomass burning, and waste incineration were developed for the year of 2014 (Qiu et al., 2016, Fu et al., 2018, Liu et al., 2018). However, the gaseous chlorine emission was not estimated in these studies. In addition, these studies did not account for the rapid decrease of coal consumption in recent years in Beijing, from 2000 Mt in 2014 to 490 Mt in 2017. More

147 importantly, the cooking source, as one of the major contributors to particulate chlorine
148 in Beijing, is not included in current chlorine emission inventories. Thus, a new
149 emission inventory of reactive chlorine species, which includes HCl, Cl_2 and PCl, were
150 developed in this study for the year of 2017.

151 The emission factor method (equation (1)) is applied to calculate the emissions of
152 these reactive chlorine species from coal combustion, biomass burning, municipal solid
153 waste incineration and industrial processes:

154 $$E_{i,j} = A_i \times EF_{i,j} \quad (1)$$

155 where $E_{i,j}$ represents the emission factor of pollutant j in sector i; A represents the
156 activity data; EF represents the emission factor. EF for PCl is estimated by $EF_{i,PCl} =$
157 $EF_{i,PM2.5} \times f_{Cl,i}$, where $f_{Cl,i}$ represents the mass fraction of PCl in primary $PM_{2.5}$.
158 Activity data are obtained from the Beijing Municipal Bureau of Statistics (available at
159 http://tjj.beijing.gov.cn/). The Cl_2 emission factor for coal combustion is calculated
160 based on the content of Cl in coal, which had been measured by Deng et al (2017). The
161 $PM_{2.5}$ emission factors and mass fractions of PCl in $PM_{2.5}$ to calculate the emissions of
162 Cl had been described in detail by Fu et al. (2018). PCl in $PM_{2.5}$ for coal combustion
163 and biomass burning are taken as 1% and 9.0%, respectively, based on local
164 measurements in Beijing.

165 Emissions of PCl from cooking, including contributions from commercial and
166 household cooking, are estimated using equation (2):

167 $$E_{PCl} = \left[N_f \times V_f \times H_f \times EF_{f,PCl} + V_c \times H_c \times N_c \times n \times EF_{c,PCl} \times (1-\eta)\right] \times 365 \quad (2)$$

168 where N_f is the number of households, V_f is the volume of exhaust gas from a household
169 stove (2000 m^3 h^{-1}); H_f is the cooking time for a family (0.5 h day^{-1}); $EF_{f,PCl}$ and
170 $EF_{c,PCl}$ are the emission factors (kg m^{-3}) of PCl for household and commercial cooking,
171 respectively; Hc is the cooking time in a commercial cooking facility (6 h day^{-1}); Nc is
172 the number of restaurants, schools and government departments. Vc is the volume of
173 exhaust gas from a commercial cooking stove (8000 m^3 h^{-1}); n is the number of stoves
174 for each unit, which equals to 6 for a restaurant and is calculated as one stove per 150
175 students for each school. η is the removal efficiency of fume scrubbers (30%). $EF_{c,PCl}$
176 is the emission factor (kg m^{-3}) of PCl in commercial cooking. These constants are all

based on Wu et al. (2018). The PCl fraction in $PM_{2.5}$ from cooking is take as 10%, based on local measurements. HCl and Cl_2 emissions from cooking are not considered in this study.

The sectoral emissions of HCl, Cl_2 and PCl are summarized in Table 1. The estimated HCl, Cl_2 and PCl emissions in Beijing are 1.89 Gg, 0.07Gg and 0.63Gg respectively. The Cl emissions estimated for 2014 by Fu et al. (2018) were used for other areas. This simplification is a good approximation because replacing coal with natural gas only occurred in Beijing, and reduction of coal consumption in surrounding regions was generally less than 15%. In addition, strict control measures for biomass burning, cooking and municipal solid waste incineration have not been implemented in most regions yet. Emissions of conventional species for this study period are developed in a separate study that is currently under review and are summarized in Table S1.

2.2 Chlorine-related heterogeneous reactions

The heterogeneous reactions in original CMAQ (version 5.0.1) are not related to chlorine species. In this study, the original heterogeneous reactions of N_2O_5 and NO_2 (R5 and R10 in Table 2) are replaced with a revised version which includes production of $ClNO_2$ from CPS (R6 and R11 in Table 2). In reaction R6, the molar yield of $ClNO_2$ (ϕ_{ClNO_2}) is represented as equation (3) (Bertram and Thornton, 2009):

$$\phi_{ClNO_2} = \left(1 + \frac{[H_2O]}{483 \times [Cl^-]}\right)^{-1} \quad (3)$$

where $[H_2O]$ and $[Cl^-]$ are the molarities of liquid water and chloride (mol m^{-3}).

In addition, laboratory observations confirmed that the heterogeneous uptake of some oxidants (such as O_3 and OH) and reactive chlorine species (such as $ClNO_2$, HOCl, and $ClONO_2$) could also occur on CPS to produce Cl_2. These reactions are implemented in the model and summarized in Table 2 as R13-R18. Note that the products from the heterogeneous uptake of $ClNO_2$ on CPS vary with particle acidity (Riedel et al., 2012; Rossi, 2003). It generates Cl_2 under the condition of pH lower than 2 but produces nitrate and chloride under higher pH conditions. The reaction rates of the heterogeneous

reactions are parameterized as first-order reactions, with the rate of change of gas phase species concentrations determined by equations (4) (Ying et al., 2015):

$$\frac{dC}{dt} = -\frac{1}{4}(v\gamma A)C = -k^{\mathrm{I}}C \tag{4}$$

where C represents the concentration of species; v represents the thermal velocity of the gas molecules (m s^{-1}); A is the CMAQ-predicted wet aerosol surface area concentration (m^2 m^{-3}); γ represents the uptake coefficient. For all gas phases species (except $ClNO_2$) involved in the heterogeneous reactions (R6 and R11-R18), a simple analytical solution can be used to update their concentrations from time t_0 to $t_0+\Delta t$: $[C]_{t0+\Delta t}=[C]_{t0}\exp(-k^{I}\Delta t)$, where Δt is the operator-splitting time step for heterogeneous reactions.

The rate of change of ClNO2 includes both removal and production terms, as shown in equation (5):

$$\begin{aligned}\frac{d[\mathrm{ClNO_2}]}{dt} &= -k_{\mathrm{i}}^{\mathrm{I}}[\mathrm{ClNO_2}] + k_6^{\mathrm{I}}\phi_{\mathrm{ClNO2}}[\mathrm{N_2O_5}] \\ &= -k_{\mathrm{i}}^{\mathrm{I}}[\mathrm{ClNO_2}] + k_6^{\mathrm{I}}\phi_{\mathrm{ClNO2}}[\mathrm{N_2O_5}]_{t0}\exp(-k_6^{\mathrm{I}}t)\end{aligned} \tag{5}$$

Assuming ϕ_{ClNO2} is a constant, an analytical solution for equation (5) can be obtained, as shown in equation (6):

$$\begin{aligned}[\mathrm{ClNO_2}]_{\mathrm{t0+\Delta t}} = {} & [\mathrm{ClNO_2}]_{\mathrm{t0}}\exp\left(-k_{\mathrm{i}}^{\mathrm{I}}\Delta t\right) \\ & + \frac{k_6^{\mathrm{I}}\phi_{\mathrm{ClNO2}}[\mathrm{N_2O_5}]_{\mathrm{t0}}}{k_{\mathrm{i}}^{\mathrm{I}} - k_6^{\mathrm{I}}}\left[\exp\left(-k_6^{\mathrm{I}}\Delta t\right) - \exp\left(-k_{\mathrm{i}}^{\mathrm{I}}\Delta t\right)\right]\end{aligned} \tag{6}$$

where $k_{\mathrm{i}}^{\mathrm{I}}$ represents the pseudo first-order rate coefficient of either reaction R17 or R18, depending on pH.

The uptake coefficients γ of gaseous species are obtained from published laboratorial studies. In the original CMAQ, the uptake coefficient of N_2O_5 is determined as a function of the concentrations of $(NH_4)_2SO_4$, NH_4HSO_4 and NH_4NO_3 (Davis et al., 2008). In this study, the PCl and NO_3^- dependent parameterization by Bertram and Thornton (2009) (equation (7)) is used:

$$\gamma_{N_2O_5} = \begin{cases} 0.02, \quad for\ frozen\ aerosols \\ 3.2\times10^{-8}K_f\left[1-\left(1+\dfrac{6\times10^{-2}[\mathrm{H_2O}]}{[\mathrm{NO_3^-}]}+\dfrac{29[\mathrm{Cl^-}]}{[\mathrm{NO_3^-}]}\right)^{-1}\right] \end{cases} \tag{7}$$

In the above equation, K_f is parameterized function based on molarity of water: $K_f =$

$1.15 \times 10^6(1 - e^{-0.13[H_2O]})$. NO_3^- and Cl^- concentrations are also in molarity. The uptake coefficient of OH is expressed in equation (8) as a function of the concentration of PCl following the IUPAC (International Union of Pure and Applied Chemistry, available at http://iupac.poleether.fr/htdocs/datasheets/pdf/O-H_halide_solutions_VI.A2.1.pdf).

$$\gamma = \min(0.04 \times \frac{[Cl^-]}{1000 \times M}, 1) \quad (8)$$

where M represents the volume of liquid water in aerosol volume ($m^3\ m^{-3}$). For frozen particles, the uptake coefficient is limited to 0.02, as used in the original CMAQ model.

The uptake coefficients of O_3, NO_3, NO_2, HOCl, $ClNO_2$, and $ClONO_2$ are treated as constants. Among of them, the γ values of NO_3, NO_2, HOCl and $ClONO_2$ are set as 3×10^{-3}, 1×10^{-4}, 1.09×10^{-3} and 0.16 based on laboratory measurements (Rudich et al., 1996; Abbatt et al., 1998; Pratte et al., 2006; Gebel et al., 2001). A preliminary value of 10^{-3} in the daytime and 10^{-5} at nighttime is chosen for the O_3 uptake coefficient. The daytime γ_{O_3} is based on the analysis of Cl_2 production rate in a hypothesized geochemical cycle of reactive inorganic chlorine in the marine boundary layer by Keene et al. (1990). The lower nighttime value was also recommended by Keene et al. (1990) who noted that Cl_2 production in the marine boundary layer are lower at night. The uptake coefficient of $ClNO_2$ depends on the particle acidity, with the value of 2.65×10^{-6} for reaction R17 and 6×10^{-3} for reaction R18 (Robert et al., 2008).

2.4 CMAQ model configuration

These heterogeneous reactions of chlorine are incorporated into a revised CMAQ based on the CMAQ version 5.0.1 to simulate the distribution of nitrate concentration in Beijing from 11 to 15 June 2017. The revised CMAQ model without heterogeneous reactions of chlorine has been described in detail by Ying et al. (2015) and Hu et al. (2016, 2017). In summary, the gas phase chemical mechanism in the revised CMAQ model is based on the SAPRC-11 (Cater et al., 2012) with a comprehensive inorganic chlorine chemistry. Reactions of Cl radical with several major VOCs, which lead to production of HCl, are also included. The aerosol module is based on AERO6 with an

updated treatment of NO_2 and SO_2 heterogeneous reaction and formation of secondary organic aerosol from isoprene epoxides. Three-level nested domains with the resolutions of 36km, 12km, and 4km using Lambert Conformal Conic projection (173×136, 135×228 and 60×66 grid cells) are chosen in this work (the domains see Figure S1). The two true latitudes are set to 25°N and 40°N and the origin of the domain is set at 34°N, 110°E. The left-bottom coordinates of the outmost domain are positioned at x = -3114 km, y = -2448 km. The BASE case (heterogeneous reactions of Cl turned off) and HET case (all heterogeneous reactions enabled) are compared to evaluate the impact of heterogeneous chlorine chemistry on nitrate formation.

3. Results

3.1 Model performance evaluation

Predicted O_3, NO_2 and $PM_{2.5}$ concentrations from the BASE case simulation are evaluated against monitoring data at 12 sites in Beijing (Table S2) in 11 to 15, June 2017. The average NMB/NME values for O_3, NO_2 and $PM_{2.5}$ across the 12 sites are -8%/29%, -7%/59% and -8%/53%, respectively. Predicted hourly Cl_2, $ClNO_2$ and N_2O_5 concentrations were compared with observations measured at the Institute of Atmospheric Physics (IAP), Chinese Academy of Sciences (39.98°N, 116.37°E) using a high-resolution time-of-flight chemical ionization mass spectrometer (CIMS) from 11 to 15 June 2017 (for site description, instrument introduction, and analytical method, please refer to the study by Zhou et al. (2018)). Figure 1 shows that the concentrations of Cl_2 and $ClNO_2$ in BASE case are rather low (close to 0), proving that the gas-phase chemistry is not the major pathway to produce Cl_2 and $ClNO_2$. By contrast, the simulated Cl_2 and $ClNO_2$ concentrations in HET case increase significantly, correspondingly the NMB and NME changes from -100% to -54% and 100% to 61% for Cl_2, and from -100% to -58% and 100% to 62% for $ClNO_2$, respectively (the particle surface area concentrations is scaled up by a factor of 5 in daytime and 10 in nighttime because this parameter is underestimated compared to the measured concentrations reported by Zhou et al. (2018)). The simulations of Cl_2 and $ClNO_2$ are improved as the

additional heterogeneous reactions prompt the production of gas phase molecular chlorine. Overall, however, the Cl_2 and $ClNO_2$ concentrations are still underestimated. Both BASE and HET simulations generally capture the hourly N_2O_5 concentrations as well as the peak values (Figure 1(c)) with similar overall NMB and NME values.

The uptake coefficient of O_3 could be an important factor affecting the predicted Cl_2 concentrations as it is found that the heterogeneous reaction of O_3 is the major source of Cl_2 during this period (see discussion in Section 3.2). The influence of different parametrizations of the uptake coefficient of N_2O_5 on $ClNO_2$ and nitrate concentrations are also discussed in Section 3.2.

Predicted NO_3^- and PCl concentrations are compared with observations measured at an adjacent monitoring site located at the rooftop of School of Environment building in Tsinghua University (THU, 40.00°N, 116.34°E, about 5 km from IAP) using an Online Analyser of Monitoring of Aerosol and Gases (MARGA) from 11 to 15 June 2017. According to Figure 1(d), the simulated nitrate concentration is slightly lower than the observations most of the time. From the evening hours of 12 June to morning hours of 13 June, observed and simulated nitrate concentration both increase significantly. The NMB and NME values of hourly nitrate for the HET case (-5% and 39%, respectively) are slightly lower than those for the BASE case -10% and 46%) during this high concentration period. The HET case also generally captures the day-to-day variation of PCl concentration and perform better than the BASE case, correspondingly the NMB and NME are reduced from -48% and 72% to -37% and 67%. The substantial underestimation of PCl in the daytime on 15 June is likely caused by missing local emissions during this period.

3.2 Impact of uptake coefficients of O_3 and N_2O_5 on chlorine species and nitrate

The uptake coefficients of O_3 and N_2O_5 may be important factors affecting the accuracy of simulated nitrate concentrations. Some studies have confirmed that the reaction of O_3 on CPS can indirectly affect the nitrate formation by increasing the atmospheric Cl_2 and OH level (Li et al., 2016; Liu et al., 2018). According to Figure 1(a), the improved model still substantially underestimates the concentration of Cl_2, which may be

associated with the underestimation of the uptake coefficients of O_3, which are empirical and have not been confirmed by laboratory studies. The uptake coefficients were increased by a factor of 10 (0.01 for daytime and 10^{-4} for nighttime) to evaluate the sensitivity of Cl_2 production and nitrate formation to this parameter. Figure 2 shows that the simulated Cl_2 and nitrate concentrations in daytime increase significantly (especially for Cl_2) and sometimes can capture the peak value (such as the daytime peak on 14 June). However, although the NMB and NME of Cl_2 and nitrate improve from -18% and 39% to 1% and 28% when the new uptake coefficients are used, the simulated Cl_2 concentrations are still quite different from the observations such as during the daytime in 11 and 12 June, see Figure 2). A non-constant parameterization of the uptake coefficients of O_3 that considers the influence of PCl concentrations, meteorology conditions, etc., similar to those of OH and N_2O_5, might be needed. Further laboratory studies should be conducted to provide a better estimation of this important parameter.

Several parameterizations for the uptake coefficient of N_2O_5 have been developed for regional and global models and have been evaluated in several previous studies (Tham et al., 2019, McDuffie et al., 2018a, 2018b). In addition to the parameterization of Bertram and Thornton (2009) used in the HET case, two additional simulations were performed to assess the impact of the uptake coefficient of N_2O_5 on nitrate formation. The first simulation uses the original CMAQ parameterization of Davis et al.(2008) and second simulation uses a constant value of 0.09, which is the upper limit of the N_2O_5 uptake coefficient derived by Zhou et al. (2018) based on observations. The results from the simulations with the parameterization of Bertram and Thornton (2009) generally agree with the results using those based on Davis et al. (2008) and the larger constant N_2O_5 leads to slightly better results, which might reflect the fact that the N_2O_5 concentrations are underestimated. Using the uptake coefficient of 0.09 can generally increase the concentration of nitrate in some periods, but it also leads to significant increase of the nitrate level (such as nighttime on 12-13 June and 13-14 June), which is 4-6 times higher than those based on Bertram and Thornton (2009). Overall, predicted nitrate concentrations are sensitive to changes in the changes in $\gamma_{N_2O_5}$, with approximately 50% increase in the nitrate when a constant of $\gamma_{N_2O_5}$ of 0.09 is used.

343 3.3 Spatial distributions of nitrate and chlorine species concentrations

344 The regional distributions of averaged Cl_2, $ClNO_2$, N_2O_5 and NO_3^- concentration from
345 11 to 15 June for the HET case are shown in Figure 3. Compared to the BASE case, the
346 episode average concentrations of Cl_2 and $ClNO_2$ from the HET case increase
347 significantly in the eastern region of Beijing, reaching up to 23 ppt and 71 ppt from
348 near zero (Figure 3a and 3b). High concentrations are not found in the southern region
349 with intensive emissions of chlorine species (Figure S2). The production of $ClNO_2$
350 requires the presence of chloride, NO_2, and O_3. In the areas close to the fresh emissions,
351 O_3 is generally low (Figure S3), and the production of NO_3 (hence N_2O_5 and $ClNO_2$) is
352 limited. Therefore, the production rate of $ClNO_2$ is generally low in areas affected by
353 fresh emissions. Since the contribution of direct emissions to Cl_2 is low and it is
354 predominantly produced secondarily in the atmosphere, high levels of Cl_2 are also
355 found away from the fresh emissions.

356 The spatial distribution of N_2O_5 concentrations differs from that of other species
357 (Figure 3c). While the concentrations of most of the species are higher in the southern
358 region, the N_2O_5 concentrations are lower in some parts of this region. This is because
359 the O_3 concentration in the core urban areas is low due to high NO_x emissions. The
360 N_2O_5 concentrations from the HET case are approximately 16% lower on average
361 (Figure 3d) because the Bertram and Thornton (2009) parameterization used in the HET
362 case generally gives higher uptake coefficients than the parameterization of Davis et al.
363 (2008) used in the BASE case (Table 3).

364 Although the higher uptake coefficients of N_2O_5 in the HET case facilitate faster
365 conversion of N_2O_5 to nitrate, the nitrate concentrations do not always increase. During
366 daytime hours, nitrate concentrations in the HET case increase due to higher OH (Figure
367 3e and Figure 3f). At nighttime, in contrast, the nitrate concentration decreases
368 significantly in some regions by about 22%, mainly due to lower molar yield of nitrate
369 from the N_2O_5 heterogeneous reaction in the HET case (Figure 3g and Figure 3h).
370 Although $ClNO_2$ produced in the N_2O_5 reaction also produces nitrate through a
371 heterogenous reaction when the particle pH is above 2, which is true for most regions
372 (see Figure S4), the uptake coefficient of $ClNO_2$ is significantly lower than that of N_2O_5

(0.01~0.09 for N_2O_5 and 6 $\times 10^{-3}$ for $ClNO_2$), leading to an overall decrease of nitrate production. As the $ClNO_2$ production from the heterogeneous reaction leads to less N_2O_5 conversion to non-relative nitrate, it may change the overall lifetime of NOx and their transport distances. The magnitude of this change and its implications on ozone and PM2.5 in local and downwind areas should be further studied.

3.4 Relationship between nitrate formation and chlorine chemistry

Nitrate productions from the homogeneous and heterogeneous pathways in Beijing are approximated by the difference in predicted nitrate concentrations between the BASE or HET case and a sensitivity case without heterogenous reactions. Averaging over the five-day period, approximately 58% of the nitrate originates from HNO_3 gas-to-particle partitioning and 42% is from heterogeneous reactions (Figure 4). This conclusion generally agrees with measurements at Peking University (PKU) (52% from the heterogeneous process and 48% from HNO_3 partitioning) on four polluted days (average in September 2016 reported by Wang et al. (2017). Slightly higher contributions of the homogeneous pathway in this study is expected because of high OH concentrations during the day and lower particle surface areas at night.

The nitrate formation from different homogeneous and heterogeneous pathways in the BASE case and HET case are further studied. Contributions of different gas phase pathways are determined using the process analysis tool in CMAQ. Contributions of different heterogeneous pathways are determined using a zero-out method that turns of one heterogeneous pathway at a time in a series of sensitivity simulations. Figure 4 shows that the reaction of OH and NO_2 is always the major pathway for the formation of nitrate through homogeneous formation of HNO_3 and gas-to-particle partitioning. However, its nitrate production rate through this homogeneous pathway decreases significantly from daytime to nighttime (from 1.81 $\mu g\ m^{-3}\ h^{-1}$ to 0.33 $\mu g\ m^{-3}\ h^{-1}$ on average). The nitrate production from other HNO_3 partitioning pathways in the daytime is negligible. At nighttime, homogeneous reaction of N_2O_5 with water vapor accounts for approximately 5% of the overall homogeneous nitrate formation. For the heterogeneous pathways, daytime production rate is approximately 0.6 $\mu g\ m^{-3}\ h^{-1}$ with

1/3 of the contributions from NO_2 and 2/3 from N_2O_5. Nighttime production on nitrate from the heterogeneous pathways is approximately 3.1 μg m^{-3} h^{-1}, of which 85% is due to N_2O_5 and 15% is due to NO_2.

Comparing the BASE case and the HET case shows that, when the chlorine chemistry is included, the gaseous HNO_3 produced by OH reacting with NO_2 increases significantly in the HET case. Correspondingly, the nitrate production rate reaches up to 2.04 μg m^{-3} h^{-1} in the daytime due to increased atmospheric OH concentrations predicted by the chlorine reactions. Similar conclusions are also obtained by Li et al. (2016) and Liu et al. (2017) based on observations and model simulations. The heterogeneous production of nitrate from the reaction of N_2O_5 uptake decreases by approximately 27% in the HET case due to the production of gas phase $ClNO_2$. According to the study by Sarwar et al. (2012; 2014), including the heterogeneous reaction of N_2O_5 with PCl decreased the nocturnal nitrate concentration by 11-21% in the United States, which was slightly less than the current study for Beijing. It is likely because PCl concentrations in the United States are significantly lower than those in Beijing (the monthly PCl concentration is 0.06 μg m^{-3} in the United State against ~1 μg m^{-3} in Beijing) so that PCl is depleted quickly. The contributions of NO_2 uptake to nitrate also decrease by 22% because of the lower rate constant of the reaction of NO_2 with PCl. In contrast, the contribution of $ClNO_2$ reacts with particle surface to nitrate production increases by 6% in the HET case. The overall nitrate concentration in the HET case is about 22% higher than that in the BASE case during this study period.

4. Conclusions

In this work, a modified CMAQ model incorporated with heterogeneous reactions for the production of molecular chlorine and other reactive chlorine species is developed and its impact on of the nitrate formation predictions are evaluated. The contributions from different homogenous and heterogeneous pathways to nitrate formation are also quantified. High concentration of Cl_2 and $ClNO_2$ do not occur in the southern part of the Beijing-Tianjin-Hebei region with intensive emissions of chlorine species as higher concentrations of O_3 and N_2O_5 associated with the heterogeneous formation of these

species generally occurred in the downwind areas. CTMs without a complete treatment of the chlorine chemistry can underestimate daytime nitrate formation from the homogeneous pathways, particularly from HNO_3 gas-to-particle partitioning due to underestimation of OH concentrations and overestimate the nighttime nitrate formation from the heterogeneous pathways due to missing chlorine heterogeneous chemistry.

Data availability. The data in this study are available from the authors upon request (shxwang@tsinghua.edu.cn)

Author contributions. XQ, QY, SW and JH designed the study; YS, BL, AS, XY provided observation data; XQ, QY, SW, JZ, QX, DD, LD and JX analyzed data. XQ, QY and SW wrote the paper.

Competing interests. The authors declare that they have no conflict of interest.

Acknowledgments. This work was supported by National Natural Science Foundation of China (21625701), China Postdoctoral Science Foundation (2018M641385), National Research Program for Key Issue in Air Pollution Control (DQGG0301, DQGG0501) and National Key R&D Program of China (2018YFC0213805, 2018YFC0214006). The simulations were completed on the "Explorer 100" cluster system of Tsinghua National Laboratory for Information Science and Technology.

References

Abbatt, J. P., Waschewsky, G. C., et al.: Heterogeneous interactions of HOBr, HNO_3, O_3, and NO_2 with deliquescent NaCl aerosols at room temperature. J. Phys. Chem, A., 102, 3719-3725, 1998.

Bertram, T. H., Thornton, J. A.: Toward a general parameterization of N_2O_5 reactivity on aqueous particles: the competing effects of particle liquid water, nitrate and chloride. Atmos. Chem. Phys., 9, 8351-8363, 2009.

Brown, S.S., Stutz, J. Nighttime radical observations and chemistry. Chemical Society Reviews, 41, 6405-6447, 2012.

Cater, W. P. L., Heo, G.: Development of revised SAPRC aromatics mechanisms. Final Report to the California Air Resources Board, Contracts No. 07-730 and 08−326, April 12, 2012

Chang, X., Wang, S., Zhao, B., et al.: Assessment of inter-city transport of particulate matter in the Beijing–Tianjin–Hebei region, Atmos. Chem. Phys., 18, 4843-4858, https://doi.org/10.5194/acp-18-4843-2018, 2018.

Davis, J. M., Bhave, P. V., Foley, K. M.: Parameterization of N_2O_5 reaction probabilities on the surface of particles containing ammonium, sulfate, and nitrate. Atmos. Chem. Phys. 8, 5295-5311, 2008.

Deng, S., Zhang, C., Liu, Y., et al.: A Full-Scale Field Study on Chlorine Emission of Pulverized Coal-Fired Power Plants in China. Research of Environmental Science. In Chinese, 27, 127-133, 2014.

Deiber, G., George, C., Le Calve, S., Schweitzer, F., Mirabel, P.: Uptake study of $ClONO_2$ and $BrONO_2$ by Halide containing droplets. Atmos. Chem. Phys. 4, 1291-1299, 2004.

Ding, D.; Xing, J.; Wang, S. X.; et al.: Emission reductions dominate the decline in the ambient $PM_{2.5}$ concentration and related mortality during 2013-2017 in China. Environ. Health Perspect., under review.

Faxon, C. B., Bean, J. K., Hildebrandt R.L.: Inland Concentrations of Cl_2 and $ClNO_2$ in Southeast Texas Suggest Chlorine Chemistry Significantly Contributes to Atmospheric Reactivity. Atmosphere, 6, 1487-1506, 2015.

Fu, X., Wang, S.X., Chang, X., et al.: Modeling analysis of secondary inorganic aerosols over China: pollution characteristics, and meteorological and dust impacts. Sci. Rep. 6, 35992, 2016.

Fu, X., Wang, T., Wang, S. X., et al.: Anthropogenic Emissions of Hydrogen Chloride and Fine Particulate Chloride in China. Environ. Sci. Technol. 52, 1644-1654, 2018.

George, I. J., Abbatt, J. P.: Heterogeneous oxidation of atmospheric aerosol particles by gas-phase radicals. Nat. Chem. 2, 713-722, 2010.

Gebel, M. E., Finlayson-Pitts, B. J.: Uptake and reaction of $ClONO_2$ on NaCl and synthetic sea salt. J. Phys. Chem. A, 105, 5178-5187, 2001.

Glasow, V.R. Wider role for airborne chlorine. Nature. 464, 168-169. 2010.

Goodman, A.L., Underwood, G.M., Grassian, V.H.: Heterogeneous reaction of NO_2: characterization of gas-phase and adsorbed products from the reaction, $2NO_2(g) + H_2O(a) \rightarrow HONO(g) + HNO_3(a)$ on Hydrated Silica Particles. The Journal of Physical Chemistry A 103, 7217-7223, 1999.

Hu, J., Chen, J., Ying, Q., Zhang, H.: One-Year Simulation of Ozone and Particulate Matter in China Using WRF/CMAQ Modeling System. Atmos. Chem. Phys. 16, 10333-10350, 2016.

Hu, J., Wang, P., Ying, Q., Zhang, H., Chen, J., Ge, X., Li, X., Jiang, J., Wang, S., Zhang,

J., Zhao, Y., Zhang, Y.: Modeling biogenic and anthropogenic secondary organic aerosol in China. Atmos. Chem. Phys. 17, 77-92, 2017.

Jobson, B. T., Niki, H., Yokouchi, Y., et al.: Measurements of C2-C6 hydrocarbons during the Polar Sunrise 1992 experiment: Evidence for Cl atom and Br atom chemistry, J. Geophys. Res., 99, 25355-25368, 1994.

Keene, W. C.; Pszenny, A. A. P.; Jacob, D. J.; Duce, R. A.; Galloway, J. N.; Schultz-Tokos, J. J.; Sievering, H.; Boatman, J. F.: The Geochemical Cycling of Reactive Chlorine through the Marine Troposphere. Global. Biogeochem., 4, 407-430, 1990.

Keene, W. C., Khalil, M. A. K., Erickson, D. J., et al.: Composite global emissions of reactive chlorine from anthropogenic and natural sources: Reactive Chlorine Emissions Inventory. J. Geophys. Res-Atmos., 104, 8429-8440, 1999.

Kleeman, M.J., Ying, Q., Kaduwela, A.: Control strategies for the reduction of airborne particulate nitrate in California's San Joaquin Valley. Atmos. Environ., 39, 5325-5341, 2005.

Knipping, E. M., Lakin, M. J., Foster, K. L., Jungwirth, P., Tobias, D. J., Gerber, R. B., Dabdub, D., Finlayson-Pitts, B. J.: Experiments and simulations of ion-enhanced interfacial chemistry on aqueous NaCl aerosols. Science, 288, 301-306, 2000.

Li, H.Y., Zhang, Q., Zheng, B., et al.: Nitrate-driven urban haze pollution during summertime over the North China Plain. Atmos. Chem. Phys.,18, 5293-5306, 2018.

Li, Q.Y., Zhang, L., Wang, T., et al. Impacts of heterogeneous uptake of dinitrogen pentoxide and chlorine activation on ozone and reactive nitrogen partitioning: improvement and application of the WRF-Chem model in southern China. Atmos. Chem. Phys.,16, 14875-14890, 2016.

Liu, X. X., Qu, H., Huey, L. G., et al.: High Levels of Daytime Molecular Chlorine and Nitryl Chloride at a Rural Site on the North China Plain. Environ. Sci. Technol., 51, 9588-9595, 2017.

Liu, Y.M., Fan, Q., Chen, X.Y.: Modeling the impact of chlorine emissions from coal combustion and prescribed waste incineration on tropospheric ozone formation in China. Atmos. Chem. Phys., 18, 2709-2724, 2018.

Ma, X.Y., Sha, T., Wang, J.Y., et al.: Investigating impact of emission inventories on $PM_{2.5}$ simulations over North China Plain by WRF-Chem. Atmos. Environ., 195, 125-140. 2018.

McDuffie, E.E., Fibiger, D.L., Dubé, W.P., et al.: Heterogeneous N_2O_5 uptake during winter: Aircraft measurements during the 2015 WINTER campaign and critical evaluation of current parameterizations. J. Geophys. Res.: Atmos., 123, 4345-4372, 2018a.

McDuffie, E.E., Fibiger, D.L., Dubé, W.P., et al.:. $ClNO_2$ yields from aircraft measurements during the 2015 WINTER campaign and critical evaluation of the current parameterization. J. Geophys.Res. Atmos., 123, 12-994, 2018b.

Osthoff, H.D., Roberts, J.M., Ravishankara, A.R.: High levels of nitryl chloride in the polluted subtropical marine boundary layer. Nat. Geosci., 1,324-328, 2008.

Pratte, P., Rossi, M. J.: The heterogeneous kinetics of HOBr and HOCl on acidified sea salt and model aerosol at 40-90% relative humidity and ambient temperature. Phys. Chem. Chem. Phys. 8, 3988-4001, 2006.

Qiu, X.H., Chai, F.H., Duan, Lei., et al.: Deriving High-Resolution Emission Inventory of Open Biomass Burning in China based on Satellite Observations. Environ. Sci. Technol., 50, 11779-11786, 2016.

Riedel, T. P.; Bertram, T. H.; Crisp, T. A.; Williams, E. J.; Lerner, B. M.; Vlasenko, A.; Li, S. M.; Gilman, J.; de Gouw, J.; Bon, D. M.; Wagner, N. L.; Brown, S. S.; Thornton, J. A., Nitryl

Chloride and Molecular Chlorine in the Coastal Marine Boundary Layer. Environ Sci Technol., 46, 10463-10470, 2012.

Roberts, J. M., Osthoff, H. D., Brown, S. S., et al.: N_2O_5 oxidizes chloride to Cl_2 in acidic atmospheric aerosol. Science, 321, 1059-1059, 2008.

Song, S.J., Gao, M., Xu, W.Q., et al.: Fine-particle pH for Beijing winter haze as inferred from different thermodynamic equilibrium models. Atmos. Chem. Phys., 18, 7423-7438, 2018.

Rossi, M J. Heterogeneous Reactions on Salts. Chemical Reviews, 103, 4823-4882, 2003.

Rudich, Y., Talukdar, R.K., Ravishankara, A.R., et al.: Reactive uptake of NO_3 on pure water and ionic solutions. J. Geophys. Res. 101, 21023-21031, 1996.

Sarwar, G., Simon, H., Bhave, P.: Examining the impact of heterogeneous nitryl chloride production on air quality across the United States. Atmospheric Chemistry and Physics, 12, 6455-6473, 2012.

Sarwar, G., Simon, H., Xing, J: Importance of tropospheric $ClNO_2$ chemistry across the Northern Hemisphere. Geophysical Research Letters, 41, 4050-4058, 2014.

Seinfeld, J.H., Pandis, S.N.: Atmospheric Chemistry and Physics: From Air Pollution to Climate Change. Wiley-Interscience, New York.2006.

Song, S. J., Gao, M., Xu, W. Q.: Fine-particle pH for Beijing winter haze as inferred from different thermodynamic equilibrium models. Atmos. Chem. Phys., 18, 7423-7438, 2018.

Spicer, C.W., Chapman, E.G., Finlayson-Pitts., et al.: Unexpectedly high concentrations of molecular chlorine in coastal air. Nature, 394, 353-356, 1998.

Thornton, J.A., Kercher, J.P., Riedel, T.P., et al.: A large atomic chlorine source inferred from mid-continental reactive nitrogen chemistry. Nature, 464, 271-274, 2010.

Tham, Y.J., Wang, Z., Li, Q., et al.: Heterogeneous N_2O_5 uptake coefficient and production yield of $ClNO_2$ in polluted northern China: roles of aerosol water content and chemical composition. Atmospheric Chemistry and Physics, 18, 13155-13171, 2018.

Tuazon, E.C., Atkinson, R., Plum, C.N., Winer, A.M., Pitts Jr., J.N.: The reaction of gas phase N2O5 with water vapor. Geophysical Research Letters 10, 953-956, 1983.

Wang, S.X., Zhao, B., Cai, S.Y., et al.: Emission trends and mitigation options for air pollutants in East Asia. Atmos. Chem. Phys., 14, 6571-6603, 2014.

Wang, H.C., Lu, K.D., Chen, X.R., et al.: High N_2O_5 concentrations observed in urban Beijing: implications of a large nitrate formation pathway. Environ. Sci. Technol. Lett. 4, 416-420, 2017.

Wen, L., Xue, L.K., Wang, X.F., et al.: Summertime fine particulate nitrate pollution in the North China Plain: increasing trends, formation mechanisms and implications for control policy. Atmos. Chem. Phys., 18, 11261-11275, 2018.

Wu, X.W., Chen, W.W., Wang, K., et al.: $PM_{2.5}$ and VOCs emission inventories from cooking in Changchun city. China Environmental Science, 38, 2882-2889, 2018.

Ying, Q., Li, J. Y., Kota, S. H.: Significant Contributions of Isoprene to Summertime Secondary Organic Aerosol in Eastern United States. Environ. Sci. Technol., 49, 7834-7842, 2015.

Young, C.J., Washenfelder, R.A., Edwards, P.M., et al.: Chlorine as a primary radical: evaluation of methods to understand its role in the initiation of oxidative cycles. Atmos. Chem. Phys. 14, 3247-3440, 2014.

Zhang, T., Peng, L., Li, Y.H.: Chemical characteristics of $PM_{2.5}$ emitted from cooking fumes. Res. Environ. Sci., 29, 183-191, 2016. In Chinese.

Zhou, W., Zhao, J., Ouyang, B., et al.: Production of N_2O_5 and $ClNO_2$ in summer in urban Beijing,

China., Atmos. Chem. Phys., 18,11581-11597, 2018.

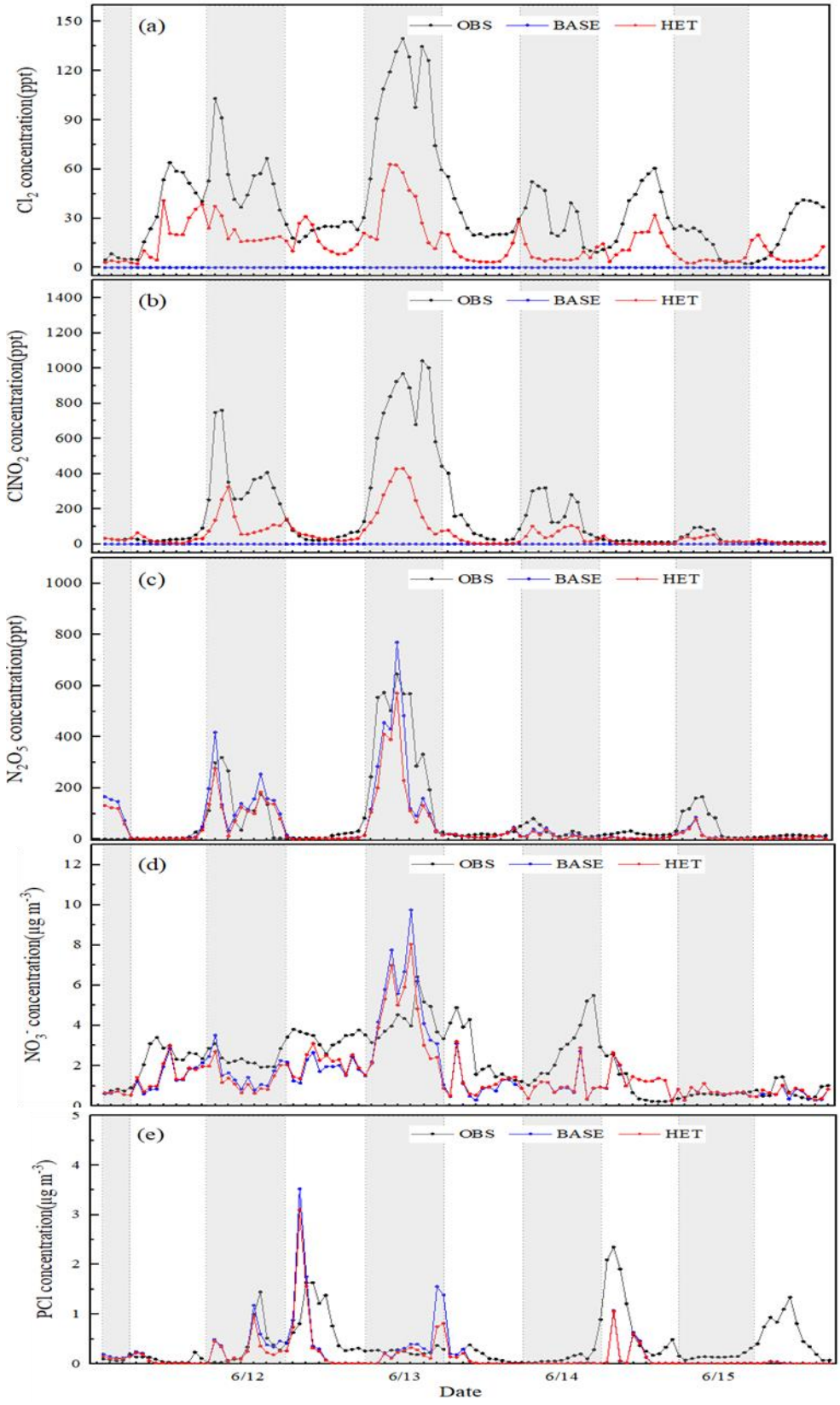

Figure 1 Comparison of observed hourly Cl_2, $ClNO_2$, N_2O_5 (at the Institute of Atmospheric Physics, Chinese Academy of Sciences), NO_3^- and PCl (at Tsinghua University) in urban Beijing with predictions from the BASE and the HET cases during 11-15 June 2017.

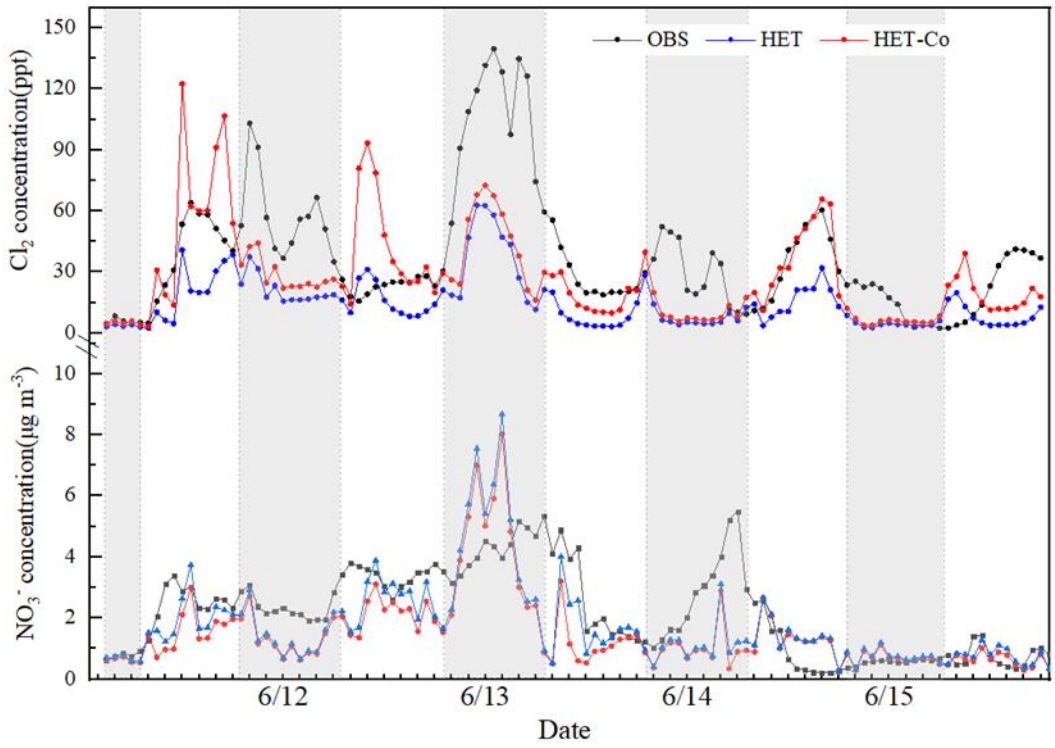

Figure 2 Comparison of observed and predicted Cl_2 and NO_3^- concentrations under different uptake coefficient of O_3 (HET: daytime $\gamma_{O_3} = 1 \times 10^{-3}$, nighttime $\gamma_{O_3} = 1 \times 10^{-5}$; HET-Co: daytime $\gamma_{O_3} = 1 \times 10^{-2}$, nighttime $\gamma_{O_3} = 1 \times 10^{-4}$).

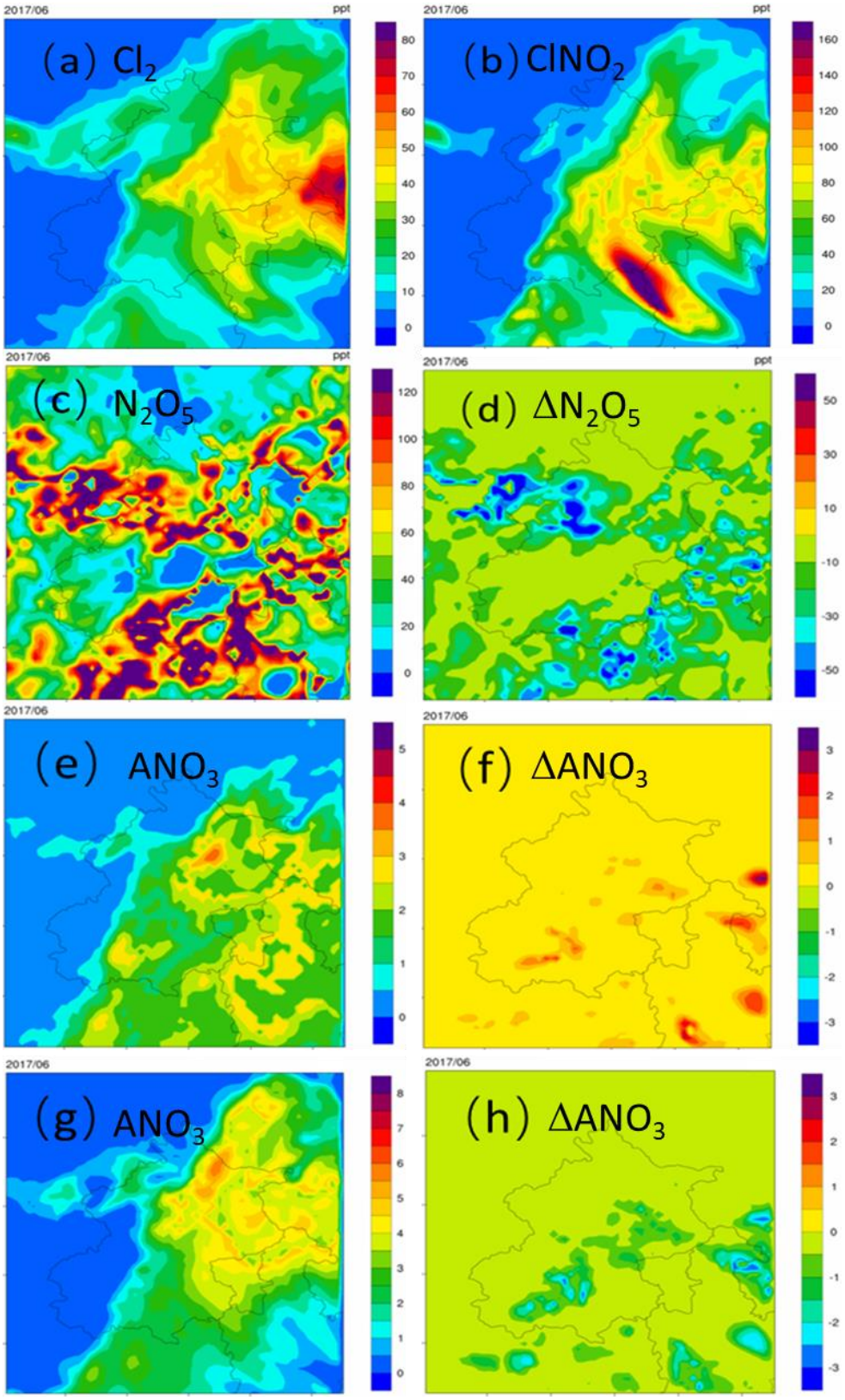

Figure 3 Spatial distributions of episode-average (a) Cl_2, (b) $ClNO_2$, (c) N_2O_5, (e) daytime (8:00 – 20:00 hours) nitrate (ANO_3) and (g) nighttime nitrate concentrations from 11-15 June 2017, and the differences in the episode-average (d) N_2O_5 (HET case – BASE case), (f) daytime nitrate and (g) nighttime nitrate. Units are μg m^{-3}.

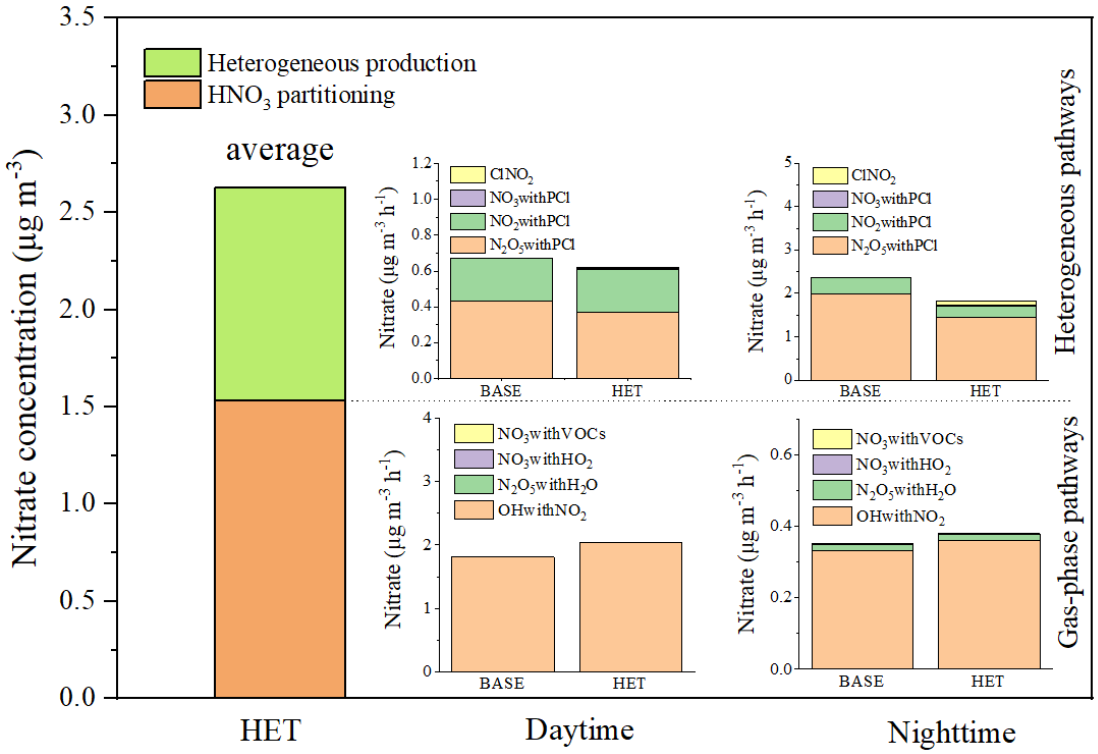

Figure 4 Contributions of different homogeneous and heterogeneous pathways to nitrate formation.

609 Table 1 The sectoral emissions of HCl, Cl_2 and PCl in Beijing in 2017. Unit: Mg year^{-1}

610

Sector	Emissions		
	HCl	Cl_2	PCl
Power plant	22.8	1.2	6.75
Industry	587.3	20.1	89.2
Residential	202.4	8.1	34.7
Biomass burning	0.182	0	0.14
Municipal solid waste	1080.2	0	8.47
Cooking	0	0	426.8
Total	1892.9	29.4	566.1

611

612

Table 2 Major gas-phase and heterogeneous pathway of producing nitrate in original CMAQ and newly added or revised heterogeneous reactions in improved CMAQ.

Type	Reactions	No.	Reference	Comment
Original CMAQ				
Gas-phase chemistry	$OH + NO_2 \rightarrow HNO_3$	R1		
	$N_2O_5 + H_2O \rightarrow 2HNO_3$	R7		
	$HO_2^{\cdot} + NO_3 \rightarrow 0.2HNO_3 + 0.8OH^{\cdot} + 0.8NO_2$	R8		
	$NO_3 + VOCs^a \rightarrow HNO_3$	R9		
Heterogeneous chemistry	$N_2O_5(g) + H_2O(aq) \rightarrow 2H^+ + 2NO_3^-$	R5		
	$2NO_2(g) + H_2O(aq) \rightarrow HONO(g) + H^+ + NO_3^-$	R10		
Improved CMAQ				
Newly added or revised heterogeneous reactions	$N_2O_5(g) + H_2O(aq) + Cl^-(aq) \rightarrow ClNO_2(g) + NO_3^-$	R6	Bertram and Thornton (2009)	Revise R5
	$2NO_2(g) + Cl^- \rightarrow ClNO(g) + NO_3^-$	R11	Abbatt et al. (1998)	Revise R10
	$NO_3(g) + 2Cl^- \rightarrow Cl_2(g) + NO_3^-$	R12	Rudich et al. (1996)	Increase NO_3^-
	$O_3(g) + 2Cl^- + H_2O(aq) \rightarrow Cl_2(g) + O_2(g) + 2OH^-$	R13	Abbatt et al. (1998)	Affect OH
	$2OH^{\cdot}(g) + 2Cl^- \rightarrow Cl_2(g) + 2OH^-$	R14	George et al. (2010)	Affect OH
	$ClONO_2(g) + Cl^- \rightarrow Cl_2(g) + NO_3^-$	R15	Deiber et al. (2004)	Affect OH
	$HOCl(g) + Cl^- + H^+ \rightarrow Cl_2(g) + H_2O$	R16	Pratte et al. (2006)	Affect OH
	$ClNO_2(g) + Cl^- + H^+ \rightarrow Cl_2(g) + HONO(g)$ (pH < 2.0)	R17	Riedel et al. (2012)	Affect OH
	$ClNO_2(g) + H_2O(aq) \rightarrow Cl^- + NO_3^- + 2H^+$ (pH ≥ 2.0)	R18	Rossi (2003)	Increase NO_3^-

[a]: presents different VOCs species. In the SAPRC-11 mechanism, the VOCs species include CCHO (Acetaldehyde), RCHO (Lumped C3+ Aldehydes), GLY (Glyoxal), MGLY (Methyl Glyoxal), PHEN (phenols), BALD (Aromatic aldehydes), MACR (Methacrolein), IPRD (Lumped isoprene product species).

Table 3 Observed day (D) and night (N) NO_3^- concentrations (Obs.) and predicted uptake coefficient of N_2O_5 (γ_{N2O5}) and nitrate concentrations (Pred.) using the parameterizations of γ_{N2O5} by Bertram and Thornton (2009) (Scenario 1), Davis et al., (2008) (Scenario 2) and the upper-limit value derived by Zhou et al. (2018) (Scenario 3)

	NO_3^-	Scenario1		Scenario2		Scenario3	
	Obs.	γ_{N2O5}	Pred.	γ_{N2O5}	Pred.	γ_{N2O5}	Pred.
06/11-D	2.54	0.033	1.59	0.008	1.32	0.09	2.17
06/11-12-N	2.42	0.043	1.67	0.037	1.37	0.09	2.12
06/12-D	3.39	0.028	2.16	0.032	2.74	0.09	3.13
06/12-13-N	4.24	0.021	4.02	0.022	4.05	0.09	6.04
06/13-D	2.57	0.012	1.18	0.008	1.06	0.09	2.47
06/13-14-N	4.10	0.022	4.45	0.022	4.45	0.09	7.13
06/14-D	0.95	0.001	1.34	0.001	1.33	0.09	1.64
06/14-15-N	2.75	0.013	1.00	0.007	0.96	0.09	2.33
06/15-D	0.75	0.001	0.66	0.001	0.66	0.09	1.11